https://doi.org/10.5194/acp-2019-742
Preprint. Discussion started: 17 September 2019


Atmospheric Chemistry and Physics Discussions

# Estimation of Cloud Condensation Nuclei number concentrations and comparison to in-situ and lidar observations during the HOPE experiments

Christa Genz[1,a,*], Roland Schrödner[1], Bernd Heinold[1], Silvia Henning[1], Holger Baars[1], Gerald Spindler[1], and Ina Tegen[1]

[1]Leibniz Institute for Tropospheric Research (TROPOS), Permoserstraße 15, 04318 Leipzig, Germany
[a]now at University of Leipzig, Institute for Meteorology (LIM), Stephanstraße 3, 04103 Leipzig, Germany
[*]previously published under the name Christa Engler

*Correspondence to:* christa.engler@uni-leipzig.de

**Abstract.** Atmospheric aerosols are the precondition for the formation of cloud droplets and have thus large influence on the microphysical and radiative properties of clouds. In this work four different methods to derive potential cloud condensation nuclei (CCN) number concentrations were analyzed and compared: A model parameterization based on simulated particle concentrations, the same parameterization based on gravimetrical particle measurements, direct CCN measurements with a CCN counter at a certain observation site and lidar derived CCN profiles. In order to allow for sensitivity studies of the anthropogenic impact, a scenario for the maximum CCN concentration under peak aerosol conditions (1985) was estimated as well. In general, the simulations are in good agreement with the observation. At ground level, an average value of around $1*10^9$ $\mathrm{CCN/m^3}$ at a supersaturation of 0.2 % was found with all methods. The discrimination of the chemical species revealed an almost equal contribution of ammonium sulfate and ammonium nitrate to the total number of potential CCN. This was not the case for the peak aerosol scenario, where almost no nitrate particles were formed. The potential activation at five different supersaturation values has been compared to the measurements. The discrepancies were lowest for the lowest and highest supersaturations, since chemical composition and the size distribution of the particles are less important in this range. In the mid supersaturation regime, the model overestimated the potentially activated particle fraction by around 30 %. The analysis of the modern (2013) and the peak aerosol scenario (1985) resulted in a scaling factor, which was defined as the quotient of the average vertical profile of the peak aerosol and present day CCN concentration. This factor was found to be around 2 close to the ground, increasing to around 3.5 between 2 and 5 km and approaching 1 (i.e., no difference between present day and peak aerosol conditions) with increasing height. By comparing the simulation with observed profiles, the vertical distribution of the potential CCN was found to be reasonable.

## 1 Introduction

Atmospheric aerosol particles play an important role in the microphysical processes of cloud formation and thus have a potentially large influence on cloud properties. However, the evaluation of their effects shows still large uncertainties (e.g., Boucher

https://doi.org/10.5194/acp-2019-742
Preprint. Discussion started: 17 September 2019


Atmospheric Chemistry and Physics Discussions

et al., 2013). In order to reduce those uncertainties, parameterizations to estimate the number concentrations of the cloud condensation nuclei (CCN) have been developed for application in models. For a realistic simulation of cloud adjustment and aerosol-cloud-interactions, a detailed representation of the aerosol in the models is required. To describe the activation of aerosol particles, the chemical composition, the number concentration and the size distribution of the aerosol particles have to be known. Parameterizations of the cloud droplet activation (e.g., Abdul-Razzak et al., 1998; Abdul-Razzak and Ghan, 2000; Petters and Kreidenweis, 2007) utilize the Köhler-Theory (Köhler, 1936) and have been implemented into regional chemistry transport models (CTM; e.g., Bangert et al., 2011; Hande et al., 2016). The influence of the aerosol composition on the droplet activation is described using the aerosol hygroscopicity, e.g., represented by the hygroscopicity parameter kappa ($\kappa$). These parameterizations enable the investigation of the interaction of the aerosol population with cloud microphysical properties.

For the regional Chemistry Transport Model (CTM) that is used in this study (COSMO-MUSCAT, see section 2.1.1), Sudhakar et al. (2017) extended the model system to allow aerosol-cloud-interactions applying the two-moment cloud microphysics scheme by Seifert and Beheng (2006). Here, the activation of aerosol particles to cloud droplets is directly considered by an online coupling of meteorology and aerosol transport. However, the aerosol is treated as bulk mass and does not explicitly consider microphysical properties. The complex consideration of aerosols and aerosol-cloud-interactions including the particle size distribution and composition in models is expensive with regard to computating time and storage and thus not feasible in particular for long-term applications.

Therefore, Hande et al. (2016) applied a combination of two existing models to produce a CCN climatology for use in limited-aera models, representing normal background conditions over Europe. First, the aerosol particle mass concentrations were simulated using a CTM with a mass-based aerosol scheme, and then the particle size distribution and the potential activation of the particles to cloud droplets were calculated offline using the parametrization of Abdul-Razzak and Ghan (2000). For applying this activation parametrization, the aerosol is assumed to be externally mixed, and the number, size and chemical composition of the aerosol particles have to be prescribed.

Measurements of the CCN number concentration in the field are valuable in order to evaluate the ability of the models to describe the activation of aerosol particles. There are several studies of in-situ observations (e.g., Henning et al., 2014; Hammer et al., 2014; Friedman et al., 2013). Also the derivation of vertical profiles of CCN with ground-based remote sensing methods is possible (e.g., Mamouri and Ansmann, 2016; Ghan et al., 2006). Direct comparisons of model results and measurements, however, are sparse.

In this study, a similar approach as in Hande et al. (2016) was applied to derive CCN from modeled aerosol distributions. It is part of the High Definition Clouds and Precipitation for advancing Climate Prediction (HD(CP)$^2$) project. The aerosol particle concentrations were simulated using the regional CTM COSMO-MUSCAT with a mass-based aerosol scheme (Wolke et al., 2012) for the periods of the (HD(CP)$^2$ Observational Prototype Experiments (HOPE), Macke et al. (2017)) in 2013 and the peak aerosol scenario for the year 1985. Afterwards, particle number size distributions and potential activation were calculated offline using the activation parametrization by Abdul-Razzak and Ghan (2000). For the potential activation of aerosol particles, their number, size, and chemical composition were taken into account. Thus, this approach is very versatile and can be applied for each type of aerosol mixture. We aim for a detailed description of the CCN abundance with three different methods: (i)

https://doi.org/10.5194/acp-2019-742
Preprint. Discussion started: 17 September 2019




model-derived, (ii) in-situ measurements, and (iii) ground-based remote sensing. The resulting CCN fields can be used in atmospheric models to analyze clouds and their radiation effects with a variable degree of complexity. This implies a fixed CCN profile, a 3D CCN field as a long-term average or even a 4D CCN field for temporary limited episodes. In detail, the following CCN datasets were compared in this study: (i) 4D parameterization based on simulated present day (year 2013) particle mass concentrations, (ii) 4D parameterization based on simulated peak emission scenario (year 1985) particle mass concentrations, (iii) parameterization based on the measured particle mass concentrations, (iv) CCN concentrations measured directly with the CCN counter, and (v) vertical CCN profiles obtained from lidar remote sensing and helicopter-borne in-situ measurements.

The manuscript is structured as follows. First, the applied CTM COSMO-MUSCAT as well as the different observation techniques are introduced and necessary assumptions are described. In section 3, the results of the comparison of CCN number concentrations obtained from the different methods are discussed. Conclusions and a summary can be found in section 4.

## 2 Methods

### 2.1 Model description

#### 2.1.1 COSMO-MUSCAT

For this study, the chemistry transport model system COSMO-MUSCAT (Wolke et al., 2012) was used. It consists of the meteorological model COSMO (COnsortium for Small scale MOdelling), which is the operational forecast model of the German Weather Service, and the chemistry transport model MUSCAT (MUltiScale Chemistry Aerosol Transport). MUSCAT is coupled to COSMO after a 24h spin-up time in each composition cycle. COSMO is driven by initial and boundary data from GME re-analysis. To ensure a realistic description of the meteorological conditions, COSMO was reinitialized every 48 hours. Both models are coupled online; the meteorology from COSMO drives the chemical transformation and atmospheric transport, treated in MUSCAT for several gas phase species and aerosol particle populations. Transport processes include advection, turbulent diffusion, sedimentation, dry and wet deposition. MUSCAT is based on mass balances, which are described by a system of time-dependent, three-dimensional advection-diffusion reaction equations. Emissions of anthropogenic primary particles and precursors of secondary aerosols are prescribed using emission fields from EMEP (European Monitoring and Evaluation Programme; EMEP (2009)). Emissions of natural primary aerosols (Saharan desert dust, primary marine aerosol particles) are computed within the model (e.g., Heinold et al., 2011), using meteorological fields (surface wind speed, precipitation) from the model itself in addition to information on surface properties read from satellite products.

### 2.2 Model setup

The study presented here is part of the High Definition Clouds and Precipitation for advancing Climate Prediction (HD(CP)$^2$) project. The main objective is to improve our understanding of clouds and precipitation, using a model for very high resolution

https://doi.org/10.5194/acp-2019-742
Preprint. Discussion started: 17 September 2019


Atmospheric Chemistry and Physics Discussions

simulations. In the ICON-LES, which is the model used in HD(CP)$^2$ (Dipankar et al., 2015; Heinze et al., 2017), there is no online aerosol transport scheme, which indicates the need of describing the aerosol and CCN offline, in order to be considered.

Model simulations covering most of Germany have been carried out for the time period of two intensive measurement campaigns during HD(CP)$^2$: HOPE, which were performed in Jülich and Melpitz, Germany. These campaigns cover the time periods between April 3 to May 31 (Jülich) and September 1 - 30, 2013 (Melpitz, see section 2.3).

The model domain investigated in this study is displayed in Fig. 1 and covers the area between 6-15°E and 48.25-54°N. The horizontal resolution was set to 7 km and the temporal resolution for the model output was set to 1h. 32 layers up to a height of 8 km were considered in the analysis. Besides the standard meteorological model output from COSMO, MUSCAT provides the mass concentrations of several gas phase species and particulate compounds.

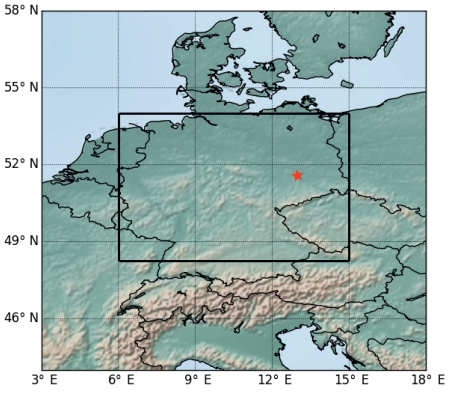


**Figure 1.** Model domain over Germany, which was used in this study. The red star marks the research station Melpitz (12.93°E, 51.53°N, 86 m a.s.l.).

### 2.2.1 Aerosol particle number estimation and CCN parametrization

Using the aerosol bulk scheme of COSMO-MUSCAT, the mass concentrations for the species considered are simulated. In order to compare the model results with in-situ particle measurements and to calculate number concentrations of potential CCN, particle number size distributions (PNSD) have to be estimated from those mass concentrations. For each species of the anthropogenic aerosol (ammonium sulfate (AS), ammonium nitrate (AN), sulfate (SU), organic (OC) and elemental carbon (EC)) and sea salt (SS), individual log-normal size distributions are assumed. The size distribution of the mineral dust (DU) particles follows a sectional scheme (Heinold et al., 2011). A log-normal size distribution is explicitly defined with the three parameters diameter or radius ($d$ or $r$, respectively), standard deviation ($\sigma$) and total number concentration ($N$). The total number concentration can be calculated from the particle mass assuming spherical particles of a certain size and density. Then, an individual geometric mean diameter and standard deviation was assumed for each considered species. The choice of geometric mean diameter and standard deviation defines the size distribution. Within the HD(CP)$^2$ framework, literature values,

https://doi.org/10.5194/acp-2019-742
Preprint. Discussion started: 17 September 2019


Atmospheric Chemistry and Physics Discussions

aerosol mass spectrometer (AMS) measurements from the TROPOS site Melpitz (Poulain et al., 2011), which is representative for central Europe (e.g., Spindler et al., 2012; Engler et al., 2007) and particle number size distribution measurements in the diameter range 10 nm to 10 µm were used to define the parameters for the log-normal distribution estimation. Adding up the log-normal size distributions of all considered species gives the total particle number size distributions. The calculations have been compared to observational data and showed a good agreement (Hande et al., 2016). The geometric mean diameter, standard deviation and density for characterizing the particle number size distributions of the individual aerosol species is listed in Tab. 1, mostly according to the values used in Hande et al. (2016).

The number and mode information of the particles could now be used to calculate the number of activated particles under certain conditions. For this purpose, the individual particle number size distributions for each considered component of the aerosol were parameterized using the hygroscopicity parameter $\kappa$ individually. The $\kappa$ values used in this study can be found in Tab. 1 as well. $\kappa$ was defined first in Petters and Kreidenweis (2007) as a single parameter to describe the relationship between the particle dry diameter, its hygroscopicity, and the CCN activation. In several laboratory studies, $\kappa$ has been determined experimentally. Highly hygroscopic particles can have a $\kappa > 1$, while for totally hydrophobic particles $\kappa = 0$. Petters and Kreidenweis (2007) reported $\kappa$ for a number of different compounds, e.g., ammonium sulfate being about 0.6 in the supersaturation regime. Further studies investigated $\kappa$ for other substances like sea salt (e.g., Niedermeier et al., 2008), coated soot (e.g., Henning et al., 2010) and secondary organic aerosol (e.g., Wex et al., 2009; Duplissy et al., 2011) or depending on the mixing state of the particles (Wex et al., 2010).

The calculation of the CCN number concentration in this study follows the parameterization of Abdul-Razzak and Ghan (2000), which relates the particle number size distribution and composition to the number of activated particles as a function of supersaturation. To achieve the maximum supersaturation (as a function of vertical velocity), accounting for particle growth before and after activation, the supersaturation balance is used. Abdul-Razzak et al. (1998) describe the parameterization for a single lognormal mode of aerosol particles (only one single species), whereas Abdul-Razzak and Ghan (2000) proposed an extended version for multiple soluble and insoluble material. Here, two (or more) particle modes compete for the available water. The same method was utilized in a previous study for parameterizing the CCN concentrations as a function of vertical velocity (Hande et al., 2016). The model is assumed to produce realistic supersaturation fields and thus also realistic CCN numbers for stratiform clouds. For convective clouds, this is different, since the sub-grid supersaturation can be much higher than the grid cell average (e.g., Hill et al., 2015).

In order to evaluate the estimations, the number concentrations of the CCN were compared to measurements close to the ground for the TROPOS super-site Melpitz. For this purpose, the same supersaturations as applied in the CCN number concentration measurements with the cloud condensation nucleus counter (CCNC, Henning et al. (2014)) were applied to the simulated particle number size distributions (see section 2.3.1).

#### 2.2.2 Estimation of peak aerosol in 1985

In order to allow for sensitivity studies of the anthropogenic impact, a peak aerosol scenario for 1985 was developed. Due to the maximum emissions of aerosols and precursor gases in Europe during the 1980s, the year 1985 was taken as a reference

https://doi.org/10.5194/acp-2019-742
Preprint. Discussion started: 17 September 2019


Atmospheric Chemistry and Physics Discussions

**Table 1.** Physical and chemical aerosol properties used in this study. The values for the particle radius and standard deviation of the size distribution follow Poulain et al. (2011) and Spindler et al. (2012) (non-dust species) and Heinold et al. (2011) (mineral dust). Several laboratory and model studies served as basis for the $\kappa$ values used in this study (Ghan et al., 2001; Petters and Kreidenweis, 2007; Wex et al., 2009; Duplissy et al., 2011).

| Species | $\kappa$ | $\sigma$ (µm) | r (µm) | $\rho$ (kgm$^{-3}$) |
|---|---|---|---|---|
| Ammonium sulfate | 0.51 | 1.6 | 0.05 | 1.77 |
| Ammonium nitrate | 0.54 | 1.6 | 0.05 | 1.725 |
| Sulfate | 1 | 1.6 | 0.05 | 1.8 |
| Sea salt 1 | 1.16 | 1.8 | 0.065 | 2.2 |
| Sea salt 2 | 1.16 | 1.7 | 0.645 | 2.2 |
| EC | 5*10$^{-7}$ | 1.8 | 0.03 | 1.8 |
| OC | 0.14 | 1.8 | 0.055 | 1.0 |
| Mineral dust 1 | 0.14 | 2.0 | 0.2 | 2.65 |
| Mineral dust 2 | 0.14 | 2.0 | 0.6 | 2.65 |
| Mineral dust 3 | 0.14 | 2.0 | 1.75 | 2.65 |
| Mineral dust 4 | 0.14 | 2.0 | 5.25 | 2.65 |
| Mineral dust 5 | 0.14 | 2.0 | 15.95 | 2.65 |

**Table 2.** Annual emissions of dust, sulfur dioxide and ammonia for entire Germany during 1985 and 2013 in Mt (UBA, 2017). So called dust also includes e.g., soot and resuspended material besides the natural mineral dust. The table also includes the factors, which the concentrations in 2013 are scaled with in order to estimate the concentrations in 1985.

| | 1985 | 2013 | ratio 1985/2013 |
|---|---|---|---|
| dust (incl. soot) | 2.65 | 0.35 | 7.7 |
| $SO_2$ | 7.73 | 0.41 | 19 |
| $NH_3$ | 0.86 | 0.74 | 1.2 |

year to compare to modern conditions. The annual emissions of sulfur dioxide and ammonia during the years 1985 and 2013 (see Tab. 2) served as basis for these estimations (UBA, 2017). In the beginning 1990s, environment protection became much more important, so efficient emission reduction strategies were developed. Furthermore, many aerosol and precursor sources simply disappeared after the liquidation of several industrie sites in Eastern Europe after the political change in 1990.

The assumptions made in order to estimate the aerosol concentrations in 1985 based on the present day simulation are summarized in Tab. 3. Particulate ammonium sulfate can be formed in the atmosphere from emitted sulfur dioxide and ammonia. In case there is still ammonia left after this reaction, ammonium nitrate can be formed as well. As can be seen from Tab. 1,

https://doi.org/10.5194/acp-2019-742
Preprint. Discussion started: 17 September 2019


Atmospheric Chemistry and Physics Discussions

**Table 3.** Assumptions for the estimation of the aerosol conditions for the 1980s over Germany.

| | 2013 | 1985 |
|---|---|---|
| Ammonium sulfate | $AS_{2013}$ | $AS_{2013}$*3.9 |
| Ammonium nitrate | $AN_{2013}$ | 0 |
| Sulfate | $SU_{2013}$ | $AS_{2013}$*5.3 |
| EC | $EC_{2013}$ | $EC_{2013}$*2 |
| OC | $OC_{2013}$ | $OC_{2013}$ |
| Sea salt | $SS_{2013}$ | $SS_{2013}$ |
| Mineral dust | $DU_{2013}$ | $DU_{2013}$ |

almost 20 times more $SO_2$ was emitted during the 1980s compared to 2013. For this reason, there was much more sulfate available in the atmosphere than necessary for the transformation of the total available ammonia to ammonium sulfate. This is why in this study the production of ammonium nitrate was set to zero and half of the additional sulfur was transformed to sulfuric acid for the 1985 scenario. This approach is encouraged by the serious "acid rain" problem in the 1980s (e.g., Seinfeld and Pandis, 1998, p. 1030ff). Since no emission data for elemental carbon in 1985 were available, the particle concentrations were assumed to be twice as high as in 2013. Organic carbon, sea salt and dust are supposed to result from natural sources and thus set to the values from 2013 in 1985 as well.

The calculations for 1985 were carried out offline with the model run from 2013 as a basis, since there was no detailed emission data for 1985 available. This implies, that the meteorological conditions of the year 1985 were not taken into account. The results have to be interpreted carefully and only as a rough estimate for the 1980s, not for spring and fall 1985 in particular. The results of the comparison of the number concentrations in 2013 and 1985, which represents the peak aerosol over Europe, are presented in section 3.

### 2.3 Measurements during HOPE

The present study utilizes observational data from the extensive measurements conducted during both HOPE campaigns at the TROPOS research station Melpitz. Additionally, at this site long-term measurements of in-situ aerosol PNSD, CCN concentrations and chemical composition of the aerosol particles are available. The rural-background site Melpitz (12.93°E, 51.53°N, 86 m a.s.l.) is located in Germany, $\sim$ 30 km east of Leipzig (Spindler et al., 2013; Engler et al., 2007) in the East German lowlands. The site at a meadow is surrounded by agricultural land. It is representative for a large area in Central Europe and long-term studies with consideration of marine or continental air mass inflow enables the investigation of the influence of different spatially distributed emission sources and long-range transport on particulate matter (PM) concentrations (Spindler et al., 2013),. The Melpitz site is integrated in the infrastructure network ACTRIS (Aerosols, Clouds, and Trace gases Research

https://doi.org/10.5194/acp-2019-742
Preprint. Discussion started: 17 September 2019


Atmospheric Chemistry and Physics Discussions

Infrastructure Network) and EMEP (Co-operative Programme for Monitoring and Evaluation of the Long-Range Transmission of Air Pollutants in Europe).

The idea behind HOPE was to gain a comprehensive dataset of observations for evaluation of the new German operational forecast model ICON (ICOsahedral Nonhydrostatic) at the scale of a couple hundred meters. The campaign focused on the convective atmospheric boundary layer, especially the connection of clouds and precipitation. Technically, HOPE aimed at combining most of the surface flux and mobile ground-based remote-sensing observations available in Germany within a single domain for the purpose of describing the vertical structure and horizontal variability of wind, temperature, humidity, aerosol particles and cloud droplets in a high temporal and spatial resolution.

In the HOPE-Melpitz campaign, in-situ observations with the helicopter-borne platform ACTOS (Airborne Cloud Turbulence Observation System) were combined with aerosol and cloud properties observed with remote sensing at the LACROS (Leipzig Aerosol and Cloud Remote Observations System) supersite. This dataset allows for the investigation of the relationship between tropospheric clouds and aerosol conditions.

Detailed information on the meteorological conditions during the two campaigns can be found in Macke et al. (2017), Tab. 3 and 4.The weather situations during HOPE-Jülich changed from a few high-pressure systems with high-level cirrus clouds, interrupted by several frontal passages (warm and cold fronts) at the beginning of the campaign, and followed by more shallow convective clouds later on. HOPE-Melpitz was dominated by low-level overcast clouds.

### 2.3.1 In-situ CCNC measurements - ground-based and airborne

Ground-based in-situ measurements with the CCNC are operational in Melpitz since August 2012 (Schmale et al., 2017) and the results were available for model evaluations within this study. The ambient CCN number concentration at Melpitz station was determined by means of size segregated activation measurements as described in detail in Henning et al. (2014), following the ACTRIS SOP (standard operating procedures, Gysel and Stratmann, 2013). Briefly, the set-up is as follows, downstream of the aerosol inlet and the drier unit, an aerosol flow of $1.5\,\mathrm{L min}^{-1}$ is size-selected with a DMPS system (Differential Mobility Particle Sizing system) and afterwards divided between a particle counter ($1\,\mathrm{L min}^{-1}$ working flow, CPC 3010, TSI Aachen Germany) and a cloud condensation nucleus counter ($0.5\,\mathrm{L min}^{-1}$ working flow, CCNC, CCN-100, Boulder, USA). With the CCNC, a stream-wise thermal gradient cloud condensation nucleus counter (Roberts and Nenes, 2005), the supersaturation-dependent activation of the particles is investigated at 0.1, 0.2, 0.3, 0.5, 0.7 and 1 % supersaturation. The ratio between the CCN number and the total particle number as counted by the CPC (condensation nuclei, CN) gives the activated fraction (AF) of the particles. This AF is calculated for each particle diameter and results in a size dependent activation curve for each supersaturation. This curve is fitted with a sigmoidal function describing the activation curve with the four parameters – lower activation limit, upper limit, sigma ($\sigma$) and the critical diameter ($D_c$). Multiplying the activation curve (CCN/CN) with the ambient size distribution integral results in the ambient CCN number concentration at the given supersaturation. One measurement per supersaturation is available every two hours.

During HOPE-Melpitz also the helicopter-borne measurement platform ACTOS was deployed (Siebert et al., 2006) in Melpitz. The experimental set-up and the flight characteristics are described in detail in Düsing et al. (2018). Within this study we

https://doi.org/10.5194/acp-2019-742
Preprint. Discussion started: 17 September 2019


Atmospheric Chemistry and Physics Discussions

use the vertically resolved in-situ data of the light weight mini cloud condensation nuclei counter (mCCNc, custom built by Gregory C. Roberts).The miniCCNc measured the CCN number concentration at a supersaturation of 0.2 %. Vertical profile measurements are available for 8 flights between Sept 12 and Sept 27 2013.

### 2.3.2 Daily $PM_{10}$ sampling at Melpitz site

Particles with aerodynamic diameter up to 10 µm ($PM_{10}$) were sampled daily at the Melpitz site. PM-High-Volume quartz filter samples for $PM_{10}$ were collected using a High-Volume sampler (DIGITEL DHA-80, Walter Riemer Messtechnik, Germany), having a sampling flux of about 30 $m^3h^{-1}$. The filter type is MK 360 quartz fibre filter (Munktell, Grycksbo, Sweden). The measurement techniques in order to determine the particle mass, water soluble ions and carbonaceous particles are described by Spindler et al. (2013, 2012). The particle mass determination was performed gravimetrically. The conditioned filters (72 hours at 20°C and 50 % relative humidity) were weighted with a microbalance as tare (blank) and after sampling of particles as gross weight. Main water-soluble ions ($NO^{3-}$, $SO_4^{2-}$, $Cl^-$, $Na^+$, $NH^{4+}$, $K^+$, $Mg^{2+}$, $Ca^{2+}$) were analyzed by ion chromatography. The determination of organic and elemental carbon (OC and EC) was performed by a two-step thermographic method using a carbon analyzer (behr Labor-Technik, Germany). OC was vaporized at 650°C for 8 minutes under nitrogen atmosphere and catalytically converted to $CO_2$ and the remaining EC was combusted further in 8 minutes with $O_2$ at 650°C. The formed $CO_2$ was than quantitatively determined by a non-dispersive infrared detector (modified VDI method 2465 part 2).

### 2.3.3 CCN concentrations derived by lidar measurements

During the HOPE campaigns, PollyXT lidar systems (Engelmann et al., 2016) were used to measure automatically and continuously the vertical state of the atmosphere in terms of aerosol particles and clouds. Lidar observations were performed in Melpitz starting September 1 until 30 2013 with the 12 channel-multiwavelength-polarization lidar PollyXT_OCEANET. Hourly averaged profiles of the particle backscatter and extinction coefficient as well as the particle depolarization ratio were calculated automatically for the whole measurement period as described in Baars et al. (2016). As the particle depolarization ratio was close to zero (indicator for spherical particles) for the whole period, one can conclude that no dust intrusion was occurring during the intensive field campaign in Melpitz. Thus, the CCN concentration profiles were calculated following the continental aerosol branch in Mamouri and Ansmann (2016).

For this approach, the lidar-derived particle backscatter profiles are converted to extinction profiles by using a lidar ratio of 50 sr as a typical value for continental sites (Baars et al., 2017). The aerosol number concentration profiles for particles with a dry radius > 50 nm ($n_{50}$) are calculated using

$$n_{50,c,dry}(z) = c_{60,c} * \sigma_c^{X_c}(z)$$

with $c_{60,c}$=25.3 $cm^{-3}$ and $X_c$=0.94 (see Mamouri and Ansmann (2016) for details). Finally, the CCN concentration at supersaturations <0.2% is estimated by multiplying $n_{50}$ with an enhancement factor of f=1. The uncertainty of this estimation is at a factor of 2-3 according to Mamouri and Ansmann (2016).

https://doi.org/10.5194/acp-2019-742
Preprint. Discussion started: 17 September 2019


Atmospheric Chemistry and Physics Discussions

**Table 4.** Average CCN number concentration ($m^{-3}$) and average contribution (%) of the considered species to the total CCN number concentration at ground level for a supersaturation of 0.2% at the HOPE site Melpitz for the 2013 campaign and the corrsponding period in 1985. The values were calculated from aerosol mass concentrations modeled with COSMO-MUSCAT. For comparison, the average value measured by the CCNC was $1.1*10^9 m^{-3}$.

| Data base / scenario | N_CCN$_{0.2\%}$, $m^{-3}$ | AS | AN | SU | EC | OC | SS | DU |
|---|---|---|---|---|---|---|---|---|
| Modeled aerosol mass concentrations (1985) | $5.2*10^9$ | 36 | 0 | 64 | 0 | 0.4 | 0.3 | 0.001 |
| Modeled aerosol mass concentrations (2013) | $9.4*10^8$ | 51 | 46 | 0.007 | 0 | 2.3 | 1.6 | 0.008 |
| Measured aerosol mass concentrations (2013) | $1.5*10^9$ | 35 | 53 | 0 | 0 | 7.4 | 0.3 | 4.0 |

## 3 Results

### 3.1 Composition of CCN

As described above, number concentrations of CCN over Germany for two time periods of the year 2013 have been calculated offline from aerosol particle number concentrations based on simulated mass concentrations of 7 different compounds: ammonium sulfate, ammonium nitrate, sulfate, organic and elemental carbon, sea salt and mineral dust. Similarly, representing a peak aerosol scenario over Europe, aerosol concentrations have been calculated for 1985 based on the simulations for the year 2013 (see section 2.2.2). Furthermore, the CCN parameterization has been applied to observed particle mass concentrations. The modeled CCN number concentrations were compared to ground-based in-situ measurements by a CCNC, and to vertical profiles derived from lidar and helicopter-borne in-situ observations at Melpitz. Table 4 lists the total number concentration of CCN and the contribution of the individual compounds as average values for the simulated time period. Nowadays, the contribution of ammonium nitrate and ammonium sulfate are almost balanced, but in the 1980s, ammonium nitrate played almost no role. The concentration of ammonium sulfate in the atmosphere was far higher than today (see also section 2.2.2), resulting in almost no ammonia being available for the formation of ammonium nitrate. Instead, much more sulfuric acid could form during this time period. Due to usage of these assumptions in the derivation of the 1985 aerosol mass concentrations, this effect can also be seen in the contributions to the CCN budget. Comparing the two different methods of estimating todays CCN concentrations, differences can be seen especially for ammonium sulfate, organic carbon and mineral dust. The dust concentrations resulting from the gravimetrical methods are usually higher than simulated, because they result from the difference of the total gravimetric mass and the sum of the masses of the individual species and are not directly measured. This is why the error is quite large due to losses of the other species during the analytical processes. Furthermore, they may contain other undetected material than only mineral dust and also re-emitted soil dust, which is not included in the emission data used in the model simulations. The difference in OC is probably due to the absence of secondary organic aerosol (SOA) in the model approach. SOA contributes a large fraction to the total concentration of organic aerosol (Jimenez et al., 2009) and also Melpitz is known to be a SOA dominated location (Poulain et al., 2011).

https://doi.org/10.5194/acp-2019-742
Preprint. Discussion started: 17 September 2019


Atmospheric Chemistry and Physics Discussions

Figure 2 shows the time series of simulated CCN for the spring and fall periods in comparison with the CCNC measurements at a supersaturation of 0.2%. The same plot is shown for a supersaturation of 0.3% in the Supplemental Figure A1. The upper panel shows the results from the model simulations while the lower one shows the results from parameterizing the gravimetrically determined particle mass concentrations. The good agreement between the CCN concentrations from the direct measurements and the estimations from chemical analytics shows, that the used CCN parametrization works reasonably well. Differences in the upper panels of Fig. 2 correspond to uncertainties in the actual aerosol simulation with the atmospheric transport model. Particularly in the first half of the spring episode, nitrate and also sulfate and thus their contribution to the CCN number concentration were clearly underestimated. In contrast, nitrate was overestimated by a factor of about 2 between day-of-year (doy) 255 and 257 (September 12-14, 2013) in the fall episode, resulting in clearly overestimated CCN numbers. This was caused by a small surface low, which was centered above the measurement station on doy 255 and then moved eastward. The location of this surface low was not correctly simulated in the model and the corresponding precipitation and thus wet deposition of aerosol particles was missing, resulting in an overestimation of particles. Furthermore, the photochemical reduction of nitrate was reduced due to cloudiness. A ridge of high pressure was following during the night of doy 257 to 258, which ended with a frontal passage and some precipitation, marking the end of this episode with clear overestimation of nitrate particles. Anyhow, since nitrate is problematic both to simulate (especially in spring) and to measure (especially in fall), the results compare satisfactorily well with the direct observation of the CCN number concentrations.

### 3.2 Comparison to in-situ CCN measurements

For a more evident comparison of the absolute number concentrations, Fig. 3 displays the simulated and measured CCN numbers at a supersaturation of 0.2% as a scatter plot for both episodes. As already seen in the time series plots in Fig. 2, the model underestimates the CCN numbers compared to both, the in-situ CCN measurements and the CCN numbers derived from the gravimetric measurements in the spring episode. In contrast, the CCN number concentration estimated from the gravimetrical measured particle mass was higher than the direct CCN measurement. For the fall episode, a better agreement between model and observation was found, except for a few outliers during two days. As mentioned above, this is probably caused by the underestimation of precipitation associated with a small low pressure system in the simulation.

In Fig. 4 the ratio of the potential CCN and the total aerosol particles (CN) larger than a certain size is shown as comparison between simulation and observation. The upper panels display the fractions for a supersaturation of 0.2% and particles larger than 110 nm for both episodes, the lower panels for a supersaturation of 0.3% and particles larger than 80 nm, respectively. A ratio of exactly one means, that as many particles would activate at the respective supersaturation as aerosol particles with a diameter larger than the threshold diameter of 110nm ($N\_CN_{110nm}$) and 80nm ($N\_CN_{80nm}$), respectively, are present in the atmosphere at this time. For the rural observation site Melpitz, this ratio is usually close to one for 0.2% and 110 nm and 0.3% and 80 nm (S. Henning, 2017, personal communication), respectively, which is why these two size threshold values were chosen for the displayed diagrams.

The $N\_CCN_{0.2\%}$ to $N\_CN_{110\,nm}$ ratios compare very well (on average 1.03 (observation) and 0.98 (model), respectively), but the model tends to overestimate the $N\_CCN_{0.3\%}$ to $N\_CN_{80\,nm}$ ratios for both episodes (on average, 0.93 (observation)

https://doi.org/10.5194/acp-2019-742
Preprint. Discussion started: 17 September 2019


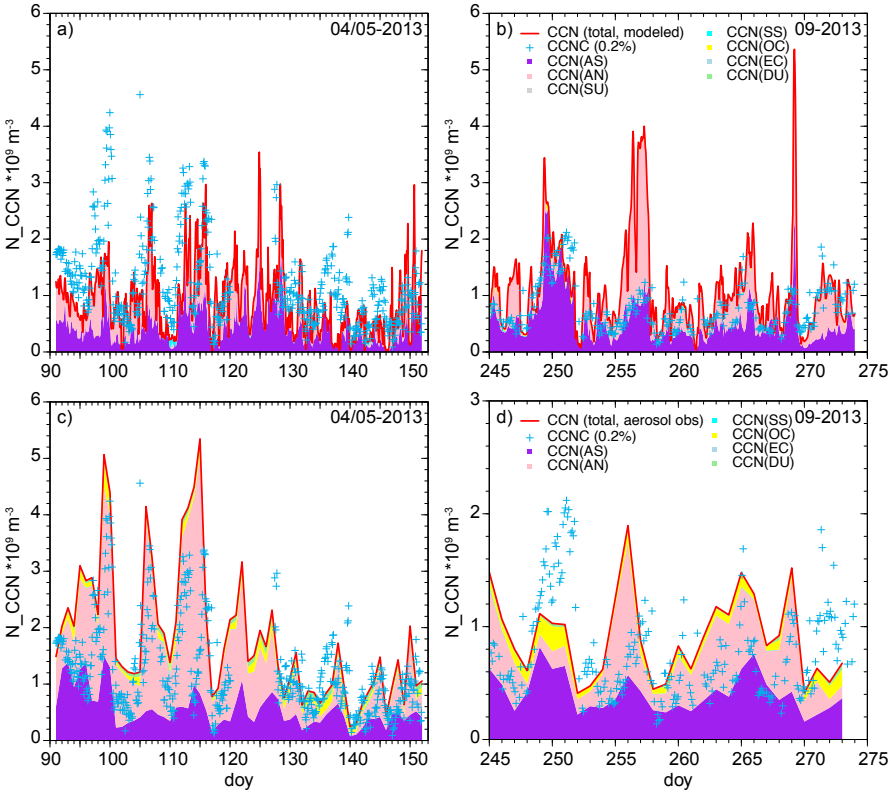


**Figure 2.** Simulated and measured CCN number concentrations in Melpitz at a supersaturation of 0.2% during HOPE-Jülich (04/05 2013) and HOPE-Melpitz (09/2013). The upper panel (a and b) shows the CCN number concentrations resulting from the simulated aerosol concentrations, the lower one (c and d) the CCN numbers resulting from measured aerosol concentrations using the same CCN parametrization. The colors represent the contributions to CCN of different species. The blue crosses indicate the CCN number concentrations using the CCNC. Please note the different time resolution for the observations, as well as the different scale for the CCN number concentration in plot d.

and 1.26 (model), respectively). This can be the result of the model either overestimating potential CCN or underestimating aerosol particle number in the size range larger than 80nm in diameter. A too large number of CCN could result from too many large particles, which activate at lower supersaturations than in the real atmosphere, or overestimated particle hygroscopicity. Since $\kappa$ is well documented in the literature, it is a less likely source of uncertainty. The detailed analysis in in Figs. 2 and A1 show that the CCN number concentration is in similar agreement with the observations for both supersaturations considered. However, as can be seen, uncertainties of the aerosol composition can lead to up to a factor of 2 difference between CCN derived from modeled and observed aerosol masses. On average, the model underestimates the CCN number by around 13% (cf. Fig. 3).

https://doi.org/10.5194/acp-2019-742
Preprint. Discussion started: 17 September 2019


Atmospheric Chemistry and Physics Discussions

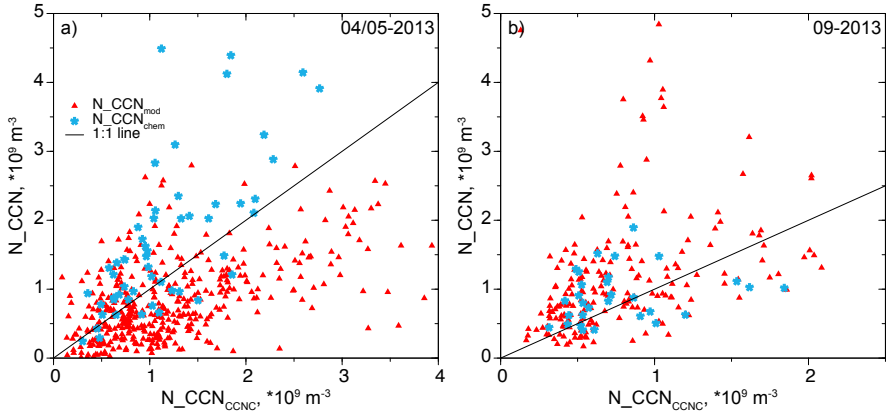


**Figure 3.** Comparison of simulated and measured CCN number concentrations in Melpitz at a supersaturation of 0.2%. Red triangles show results from the aerosol simulations, green stars result from applying the CCN parameterization to the chemically measured particle concentrations.

Due to the assumptions made to transfer modeled aerosol mass into number size distributions (see Tab. 1) the usually large number of particles in the Aitken or even nucleation range cannot be considered. As already shown by Hande et al. (2016), with this approach the number concentration of CN particles larger than 110 nm compares well with the measurements. On average, the model underestimates these numbers by less than 10%. However, this is different for smaller particle size ranges, e.g., the total number of particles larger than 80 nm is underestimates by 35% (Hande et al., 2016). Hence, the underestimated modeled number concentration of aerosol particles in the size range between 80 and 110 nm in diameter is the main reason for the different behavior between the $N\_CCN_{0.2\%}$ to $N\_CN_{110\,nm}$ ratio and the $N\_CCN_{0.3\%}$ to $N\_CN_{80\,nm}$ ratio.

Fig. 5 shows the average N_CCN-to-N_CN ratio for five different supersaturations between 0.1 and 0.7% for a cut-off diameter of 40 nm. It can be seen from this graph, that at a low supersaturation of 0.1%, only very few particles activate, whereas almost all particles activate at a high supersaturation of 0.7%. In the model, more of the available aerosol particles activate at a respective supersaturation, which is most pronounced in the medium range of supersaturations.

### 3.3 Evaluation of the vertical structure of CCNs

In order to evaluate the vertical distribution of the CCN concentrations and investigate its change since the 1980s, the modeled vertical profiles are compared to measurements. Figure 6 shows a comparison of the CCN number concentration vertical profiles over the two months spring episode in 2013 over Melpitz as simulated with COSMO-MSUCAT and derived from lidar (6 a) and ACTOS in-situ (6 b) observations. Displayed are the median values as well as the 0.25- and 0.75-quantiles. Close to the ground, the model compares quite well to the two observations. The average CCN number concentration is overestimated by less than 50%, which is in the range of the observation uncertainty of up to a factor of 2. At a height of around 1.3 km the observed and measured CCN concentrations start to decrease considerably, but clearly most strongly in the lidar observations. In contrast to the model, the CCN number concentration derived from the lidar are on average negligible at heights above 4 km.

https://doi.org/10.5194/acp-2019-742
Preprint. Discussion started: 17 September 2019


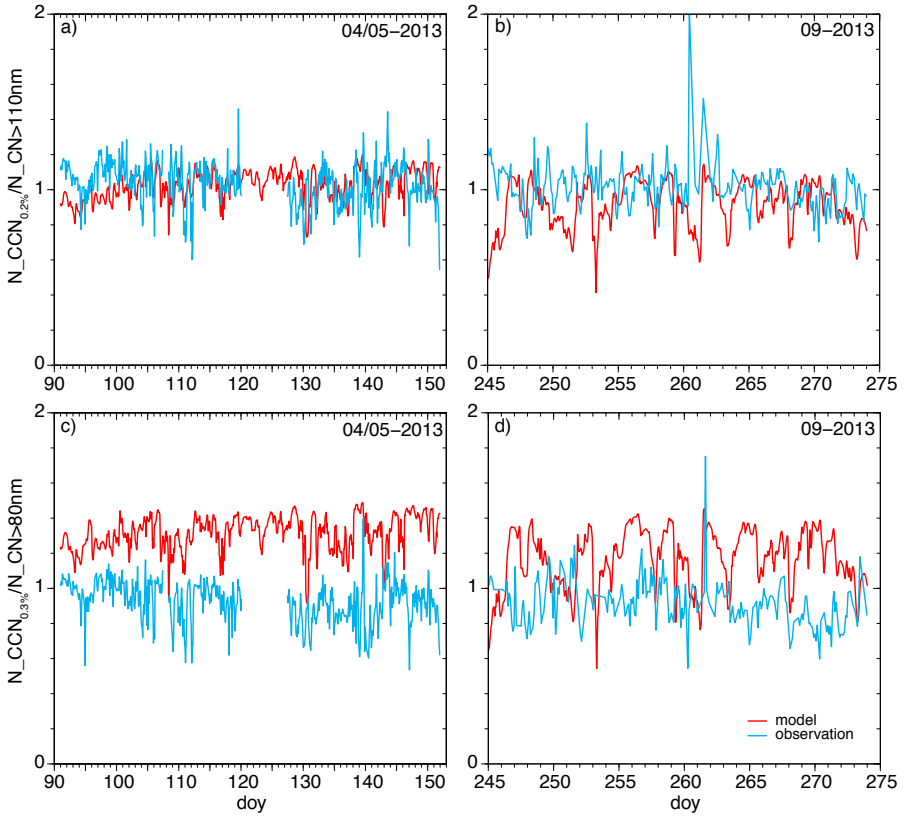


**Figure 4.** Comparison of the modeled and observed activated fraction (N_CCN/N_CN) at a supersaturation of 0.2% (a and b) and 0.3% (c and d), respectively. As number of total CN, the number concentration of CN>110 nm (a and b) and >80 nm (c and d), respectively, was used.

Nevertheless, the variability of the observed CCN number concentrations is higher in the free troposphere. This is mainly an expression of considerably increased detection uncertainty. Overall, the modeled present day-CCN number concentration is in-line with the observations, whereas the estimated profile for the 1980s is far outside today's observational range (cf. Figs. 6 and **??**). This clearly shows the influence of anthropogenic air pollution on the CCN number.

### 3.4 Present day and historic vertical CCN profiles

For each of the two evaluation periods, a temporally and spatially averaged vertical profile of the CCN concentration was calculated for the year 2013 and 1985 emission scenario, which is displayed together with the 0.05, 0.25, 0.75 and 0.95 quantiles in Fig. 7 a - d. For the calculation, a vertical velocity of 1 $\mathrm{ms}^{-1}$ was assumed. The shape and values of the profiles show no major differences for the spring and fall episode. Close to the ground, where aerosol particles are emitted, the number concentrations of potential CCN are higher than in the free troposphere. With increasing height, the number of aerosol particles and thus also that of potential CCN is decreasing. This is the case for both the 2013 and 1985 scenario. In 2013, the concentrations are

https://doi.org/10.5194/acp-2019-742
Preprint. Discussion started: 17 September 2019


Atmospheric Chemistry and Physics Discussions

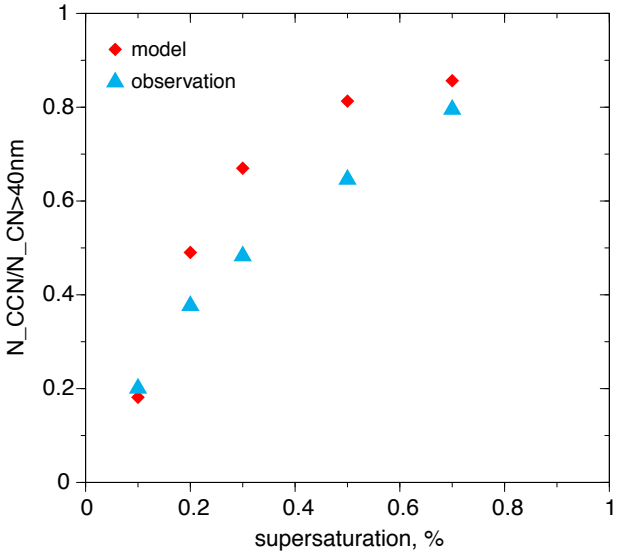


**Figure 5.** Simulated and observed fraction of potential CCN to total particle number concentration with a diameter larger than 40nm (N_CCN/N_CN) as a function of supersaturation.

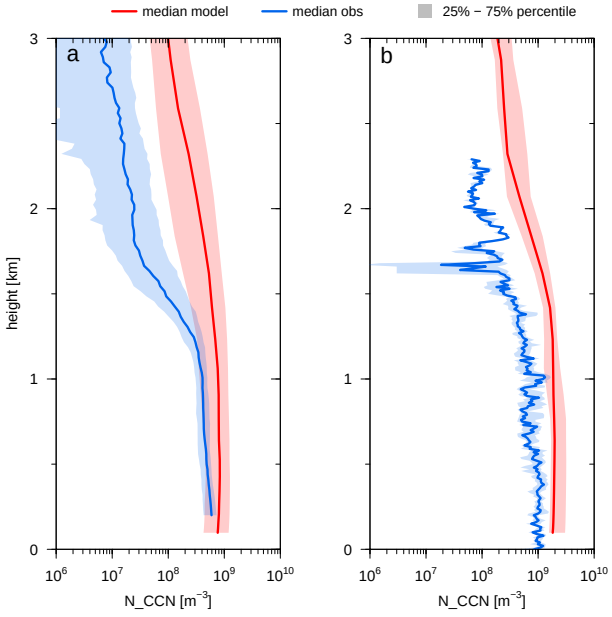


**Figure 6.** Comparison of the simulated CCN number concentration vertical profiles (red) to profiles derived from observations (blue) of (a) lidar (04/05 2013) and (b) ACTOS (09/2013) over Melpitz. The shading depicts the range between the 0.25- and the 0.75-quantile.

https://doi.org/10.5194/acp-2019-742
Preprint. Discussion started: 17 September 2019


Atmospheric Chemistry and Physics Discussions

almost constant up to a height of 1 km (around 1.0*$10^9$ $m^{-3}$) due to the well mixed boundary layer and decrease above (Fig. 7 a, d). This is less pronounced in the year 1985 simulations (Fig. 7 c, d), in which the concentrations close to the ground are much higher (around 3*$10^9$ $m^{-3}$) and decrease almost immediately with height. At the top of the uppermost simulated layer (8 km), similar concentrations of 5*$10^7$ to 1*$10^8$ $m^{-3}$ were found for both, the present day and peak aerosol scenario. Due to different aerosol composition and, hence, aerosol hygroscopicity between 1985 and 2013, the shape of the CCN profiles in the two scenarios differs. Based on the CCN profiles, a scaling factor for the CCN concentration was calculated, which varies with height (Fig. 7 c, f). This scaling factor describes the mean temporal trend of the CCN number concentration between past peak aerosol in the 1980s and present day conditions in Europe and can easily be used for sensitivity studies. The difference in the height dependency of the number concentrations between the 2013 and 1985 simulations is the reason for the bend in the scaling factor at around 1 km height (Fig. 7 e, f), because at this height, also the concentrations in the 2013 simulations start to decrease. Close to the ground, a factor of around two was found. The efficacy of pollution reduction policies and the breakdown of industrial production in Eastern Europe since the 1980s becomes evident, in relative terms, most pronounced in the height between 2 and 5 km, where a scaling factor of up to a factor of 3.5 was found. In the upper troposphere, the scaling factor decreases to around one, which means there is no difference between the 1980s and present day concentrations.

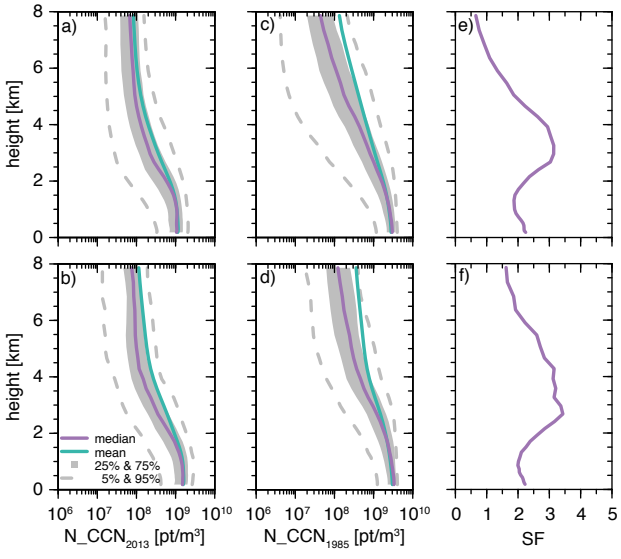


**Figure 7.** Spatial and temporal averaged vertical profile of the CCN number concentration as computed by COSMO-MUSCAT for the spring and fall period in 2013 (a and b), the estimation for the 1985 peak aerosol scenario (c and d) and scaling factor (SF) for the two scenarios (SF=$N\_CCN_{1985}$ / $N\_CCN_{2013}$; e and f).

https://doi.org/10.5194/acp-2019-742
Preprint. Discussion started: 17 September 2019


Atmospheric Chemistry and Physics Discussions

## 4 Summary and conclusions

The CCN number concentrations from different simulation estimates and observation techniques were compared in this study for the period of the HOPE field experiment in Germany in spring and fall 2013. Based on simulations of the mass concentrations of different aerosol species (ammonium sulfate, ammonium nitrate, sulfate, organic carbon, elemental carbon, sea salt, and mineral dust) using the regional CTM COSMO-MUSCAT, the CCN number was parametrized offline using a state-of-the-art parameterization for cloud droplet activation. The resulting CCN number concentrations were compared to (i) direct CCN measurements with a CCN counter, (ii) CCN number concentrations derived from applying the activation parameterization to gravimetrically measured aerosol concentrations, and (iii) to vertical profiles derived from lidar and helicopter-borne in-situ measurements. In addition, CCN number concentrations were computed based on the COSMO-MUSCAT simulations for the corresponding period in the year 1985, when industrial air pollution in Europe had peaked. Comparing the year 2013 and 1985 results allows to investigate the impact of anthropogenic air pollution and the potential of reduction measures on the atmospheric CCN budget.

The quality of the modeled CCN number concentrations is defined by both, the quality of the aerosol particle simulation and the CCN parametrization. From the good agreement between CCN derived from gravimetrical measurements and CCNC measurements, it can be concluded that the cloud droplet activation and growth parameterization gives reasonable results. Discrepancies of the offline CCN calculation from the model simulations can then be concluded resulting mostly from uncertainties in the modeled aerosol mass and composition as well as the assumptions for the transfer from particle mass into number size distribution. The comparison of the ratio of the CCN number concentration and the total particle number of particles larger than 110 $\mathrm{nm}$ in diameter shows a good agreement between model and observation for 0.2 $\%$ supersaturation. However, for supersaturations between 0.2 $\%$ and 0.7 $\%$ and smaller threshold sizes to define CN (e.g., particles larger than 40 $\mathrm{nm}$), the model overestimates the activated particle fraction. Since the assumed size distributions focus on the correct prediction of accumulation mode particles, which are the most relevant for deriving CCN number concentrations, the number of particles smaller than $\sim$100 $\mathrm{nm}$ is very likely underrepresented.

The vertical structure of the simulated CCN number concentration was also shown to agree reasonably well with ground-based remote sensing and airborne in-situ measurements, even though the variability could not be reproduced by the model. Close to the ground, model and observation agree well, but the measurement based profiles show a much larger range, which is probably due to both, a high variability in the real atmosphere during the two months of the experiment and measurement uncertainties (factor 2-3). In conclusion, the simulated profiles of the present-day simulation are within the variability range of the measurement-based profiles and thus represent realistic conditions. The 1985 simulation, however, has much larger CCN number concentration far outside the variability range of the present-day observations, as expected. A vertical-resolved scaling factor between the 2013 and 1985 results was computed, which is well suited for application in model sensitivity studies.

The scaling factor for estimating peak aerosol concentrations during the 1980s from current simulations is not vertically homogeneous. Close to the ground, a factor of 2 was determined, increasing to 3.5 between 2 and 5 $\mathrm{km}$ height. Here the effect of strict emission reduction policies and reduction in industrial production in Eastern Europe especially in the 1990s becomes

https://doi.org/10.5194/acp-2019-742
Preprint. Discussion started: 17 September 2019


Atmospheric Chemistry and Physics Discussions

apparent. Towards the upper troposphere at around 8 km height, the factor decreases again to 1. This means, the dynamics of the troposphere have a large influence on the distribution of the aerosol particles and thus the CCN distribution. Especially the height range of 2 to 5 km, where a very high CCN number concentration during the 1980s was found, is important for cloud and precipitation formation in the mid-latitudes. A significantly higher number of CCN points to large differences in the cloud droplet number concentration and thus the radiative properties of the clouds as well as in the precipitation probability during that time. The analysis of the radiative impacts including effects on cloud cover and albedo effects are subject of future studies.

*Data availability.* Data used in this manuscript can be provided upon request by email to the corresponding author, Christa Genz (christa.engler@uni-leipzig.de).

https://doi.org/10.5194/acp-2019-742
Preprint. Discussion started: 17 September 2019


Atmospheric Chemistry and Physics Discussions

## Appendix A

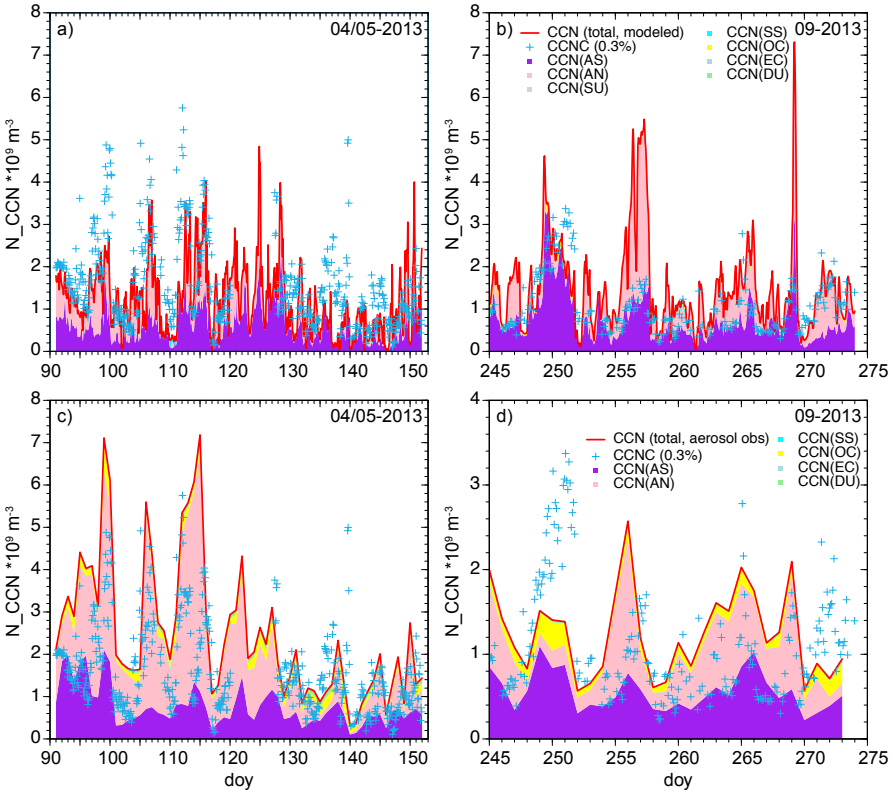


**Figure A1.** Simulated and measured CCN number concentrations in Melpitz at a supersaturation of 0.3% during HOPE-Jülich (04/05 2013) and HOPE-Melpitz (09/2013). The upper panel (a and b) shows the CCN number concentrations resulting from the simulated aerosol concentrations, the lower one (c and d) the CCN numbers resulting from measured aerosol concentrations using the same CCN parametrization. The colors represent the contributions to CCN of different species. The blue crosses indicate the CCN number concentrations using the CCNC. Please note the different time resolution for the observations, as well as the different scale for the CCN number concentration in plot d.

*Author contributions.* Christa Genz working with Ina Tegen and Bernd Heinold ran the COSMO-MUSCAT model, and performed the aerosol evaluation and CCN concentration calculation. Roland Schrödner joined the analysis of the CCN concentration profiles. Silvia Henning provided the CCNC measurements, Holger Baars the lidar derived CCN profiles and Gerald Spindler obtained the chemical measurements and analysis. Christa Engler prepared the manuscript with contributions from all co-authors.

https://doi.org/10.5194/acp-2019-742
Preprint. Discussion started: 17 September 2019


Atmospheric Chemistry and Physics Discussions

*Competing interests.* The authors declare that they have no conflict of interest.

*Acknowledgements.* This work was funded by the Federal Ministry of Education and Research in Germany (BMBF) through the research programme "High Definition Clouds and Precipitation for Climate Prediction - HD(CP)$^2$" (FKZ: 01LK1503F. The authors wish to thank Luke Hande for providing a version of CCN-calculation code, which served as basis for the estimations shown here. We also acknowledge good cooperation and support from the German Weather Service (Deutscher Wetterdienst, DWD) and the high performance computing center Jülich.

https://doi.org/10.5194/acp-2019-742
Preprint. Discussion started: 17 September 2019


Atmospheric Chemistry and Physics Discussions

## References

Abdul-Razzak, H. and Ghan, S.: A parametreization of aerosol activation: 2. Multiple aerosol types, Journal of Geophysical Research, 105, 2000.

Abdul-Razzak, H., Ghan, S., and Rivera-Carpio, C.: A parametreization of aerosol activation: 1. Single aerosol types, Journal of Geophysical Research, 103, 6123–6131, 1998.

Baars, H., Kanitz, T., Engelmann, R., Althausen, D., Heese, B., Komppula, M., Preißler, J., Tesche, M., Ansmann, A., Wandinger, U., Lim, J.-H., Ahn, J., Stachlewska, I., V, A., Marinou, E., Seifert, P., Hofer, J., Skupin, A., Schneider, F., Bohlmann, S., Foth, A., Bley, S., Pfüller, A., Giannakaki, E., Lihavainen, H., Viisanen, Y., Hooda, R., Pereira, S., Bortoli, D., Wagner, F., Mattis, I., Janicka, L., Markowicz, K., Achtert, P., Artaxo, P., Pauliquevis, T., Souza, R., van Zyl, V. S. P., Beukes, J., Sun, J., Rohwer, E., Deng, R., Mamouri, R.-E., and Zamorano, F.: An overview of the first decade of Polly$^{NET}$: an emerging network of automated Raman-polarization lidars for continuous aerosol profiling, Atmospheric Chemistry and Physics, 16, 5111–5137, 2016.

Baars, H., Seifert, P., Engelmann, R., and Wandinger, U.: Target categorization of aerosol and clouds by continuous multiwavelength-polarization lidar measurements, Atmospheric Measurements Techniques, 10, 3175–3201, doi:10.5194/amt-10-3175-2017, 2017.

Bangert, M., Kottmeier, C., Vogel, B., and Vogel, H.: Regional scale effects of the aerosol cloud interaction simulated with an online coupled comprehensive chemistry model, Atmospheric Chemistry and Physics, 11, 4411–4423, doi:10.5194/acp-11-4411-2011, 2011.

Boucher, O., Randall, D., Artaxo, P., Bretherton, C., Feingold, G., Forster, P., Kerminen, V.-M., Kondo, Y., Liao, H., Lohmann, U., Rasch, P., Satheesh, S., Sherwood, S., X., B. S., and Zhang: Clouds and Aerosols, in: Climate Change 2013: The Physical Science Basis. Contribution of Working Group I to the Fifth Assessment Report of the Intergovernmental Panel on Climate Change, Cambridge Univ Press, New York, 2013.

Dipankar, A., Stevens, B., Heinze, R., Moseley, C., Zängl, G., Giorgetta, M., and Brdar, S.: Large eddy simulation using the general circulation model ICON, Journal of Advances in Modeling Earth Systems, 7, 963–986, 2015.

Duplissy, J., DeCarlo, P., Dommen, J., Alfarra, M., Metzger, A., Barmpadimos, I., Prevot, A., Weingartner, E., Tritscher, T., Gysel, M., Aiken, A., Jimenez, J., Canagaratna, M., Worsnop, D., Collins, D., Tomlinson, J., and Baltensperger, U.: Relating hygroscopicity and composition of organic aerosol particulate matter, Atmospheric Chemistry and Physics, 11, 1155–1165, 2011.

Düsing, S., Wehner, B., Seifert, P., Ansmann, A., Baars, H., Ditas, F., Henning, S., Ma, N., Poulain, L., Siebert, H., Wiedensohler, A., and Macke, A.: Helicopter-borne observations of the continental background aerosol in combination with remote sensing and ground-based measurements, Atmospheric Chemistry and Physics, 18, 1263–1290, doi:10.5194/acp-18-1263-2018, https://www.atmos-chem-phys.net/18/1263/2018/, 2018.

EMEP: European Monitoring and Evaluation Programme, http://www.emep.int/, 2009.

Engelmann, R., Kanitz, T., Baars, H., Heese, B., Althausen, D., Skupin, A., Wandinger, U., Komppula, M., Stachlewska, I., Amiridis, V., Marinou, E., Mattis, I., Linné, H., and Ansmann, A.: The automated multiwavelength Raman polarization and water-vapor lidar Polly$^{XT}$: the neXT generation, Atmospheric Measurement Techniques, 9, 1767–1784, 2016.

Engler, C., Rose, D., Wehner, B., Wiedensohler, A., Brüggemann, E., Gnauk, T., Spindler, G., Tuch, T., and Birmili, W.: Size distributions of non-volatile particle residuals (Dp < 800nm) at a rural site in Germany and relation to air mass origin, Atmospheric Chemistry and Physics, 7, 5785–5802, 2007.

https://doi.org/10.5194/acp-2019-742
Preprint. Discussion started: 17 September 2019


Atmospheric Chemistry and Physics Discussions

Friedman, B., Zelenyuk, A., Beranek, J., Kulkarni, G., Pekour, M., Hallar, A. G., McCubbin, I., Thornton, J., and Cziczo, D.: Aerosol measurements at a high-elevation site: composition, size, and cloud condensation nuclei activity, Atmospheric Chemistry and Physics, 13, 11 839–11 851, doi:10.5194/acp-13-11839-2013, 2013.

Ghan, S., Laulainen, N., Easter, R., Wagener, R., Nemesure, S., Chapman, E., Zhang, Y., and Leung, R.: Evaluation of aerosol direct radiative forcing in MIRAGE, Journal of Geophysical Research, 106, 5295–5316, 2001.

Ghan, S., Rissman, T., Elleman, R., Ferrare, R., Turner, D., Flynn, C., Wang, J., Ogren, J., Hudson, J., Jonsson, H., VanReken, T., Flagan, R., and Seinfeld, J.: Use of in situ cloud condensation nuclei, extinction, and aerosol size distribution measurements to test a method for retrieving cloud condensation nuclei profiles from surface measurements, Journal of Geophysical Research, 111, D05S10, doi:10.1029/2004JD005752, 2006.

Gysel, M. and Stratmann, F.: WP3 - NA3: In-situ chemical, physical and optical properties of aerosols, http://www.actris.net/Publications/ACTRISQualityStandards/tabid/11271/language/en-GB/Default.aspx, 2013.

Hammer, E., Bukowiecki, N., Gysel, M., Jurányi, Z., Hoyle, C., Vogt, R., Baltensperger, U., and Weingartner, E.: Investigation of the effective peak supersaturation for liquid-phase clouds at the high-alpine site Jungfraujoch, Switzerland (3580ma.s.l.), Atmospheric Chemistry and Physics, 14, 1123–1139, doi:10.5194/acp-14-1123-2014, 2014.

Hande, L., Engler, C., Hoose, C., and Tegen, I.: Parameterizing cloud condensation nuclei concentrations during HOPE, Atmospheric Chemistry and Physics, 16, 12 059–12 079, 2016.

Heinold, B., Tegen, I., Schepanski, K., Tesche, M., Esselborn, M., Freudenthaler, V., Gross, S., Kandler, K., Knippertz, P., and Müller, D.: Regional modeling of Saharan dust and biomass-burning smoke, Tellus B, 63, 781–799, 2011.

Heinze, R., Moseley, C., Böske, L., Muppa, S., Maurer, V., Raasch, S., and Stevens, B.: Evaluation of large-eddy simulations forced with mesoscale model output for a multi-week period during a measurement campaign, Atmospheric Chemistry and Physics, 17, 7083–7109, 2017.

Henning, S., Wex, H., Hennig, T., Kiselev, A., Snider, J., Rose, D., Dusek, U., Frank, G., Pöschl, U., Kristensson, A., Bilde, M., Tillmann, R., Kiendler-Scharr, A., Mentel, T., Walter, S., Schneider, J., Wennrich, C., and Stratmann, F.: Soluble mass, hygroscopic growth, and droplet activation of coated soot particles during LACIS Experiment in November (LExNo), Journal of Geophysical Research, 115, doi:10.1029/2009JD012 626, 2010.

Henning, S., Dieckmann, K., Ignatius, K., Schäfer, M., Zedler, P., Harris, E., Sinha, B., van Pinxteren, D., Mertes, S., Birmili, W., Merkel, M., Wu, Z., Wiedensohler, A., Wex, H., Herrmann, H., and Stratmann, F.: Influence of cloud processing on CCN activation behaviour in the Thuringian Forest, Germany during HCCT-2010, Atmospheric Chemistry and Physics, 14, 7859–7868, doi:doi:10.5194/acp-14-7859-2014, 2014.

Hill, P., Morcrette, C., and Boutle, I.: A regime-dependent parameterization of subgrid-scale cloud water content variability, Quarterly Journal of the Royal Meteorological Society, 141, 1975–1986, 2015.

Jimenez, J., Canagaratna, M., Donahue, N., Prevot, A., Zhang, Q., Kroll, J., DeCarlo, P., Allan, J., Coe, H., Ng, N., Aiken, A., Docherty, K., Ulbrich, I., Grieshop, A., Robinson, A., Duplissy, J., Smith, J., Wilson, K., Lanz, V., Hueglin, C., Sun, Y., Tian, J., Laaksonen, A., Raatikainen, T., Rautiainen, J., Vaattovaara, P., Ehn, M., Kulmala, M., Tomlinson, J., Collins, D., Cubison, M., Dunlea, E., Huffman, J., Onasch, T., Alfarra, M., Williams, P., Bower, K., Kondo, Y., Schneider, J., Drewnick, F., Borrmann, S., Weimer, S., Demerjian, K., Salcedo, D., Cottrell, L., Griffin, R., Takami, A., Miyoshi, T., Hatakeyama, S., Shimono, A., Sun, J., Zhang, Y., Dzepina, K., Kimmel, J., Sueper, D., Jayne, J., Herndon, S., Trimborn, A., Williams, L., Wood, E., Middlebrook, A., Kolb, C., Baltensperger, U., and Worsnop, D.: Evolution of Organic Aerosols in the Atmosphere, Science, 326, 1525–1529, 2009.

https://doi.org/10.5194/acp-2019-742
Preprint. Discussion started: 17 September 2019


Atmospheric Chemistry and Physics Discussions

Köhler, H.: The nucleus in and the growth of hygroscopic droplets, Transactions of the Faraday Society, 32, 1152–1161, 1936.

Macke, A., Seifert, P., Baars, H., Barthlott, C., Beekmans, C., Behrendt, A., Bohn, B., Brueck, M., Bühl, J., Crewell, S., Damian, T., Deneke, H., Düsing, S., Foth, A., Girolamo, P. D., Hammann, E., Heinze, R., Hirsikko, A., Kalisch, J., Kalthoff, N., Kinne, S., Kohler, M., Löhnert, U., Madhavan, B. L., Maurer, V., Muppa, S. K., Schween, J., Serikov, I., Siebert, H., Simmer, C., Späth, F., Steinke, S., Träumner, K., Trömel, S., Wehner, B., Wiesner, A., Wulfmeyer, V., and Xie, X.: The HD(CP)$^2$ Observational Prototype Experiment (HOPE) - an overview, Atmospheric Chemistry and Physics, 17, 4887–4914, 2017.

Mamouri, R. E. and Ansmann, A.: Potential of polarization lidar to provide profiles of CCN- and INP-relevant aerosol parameters, Atmospheric Chemistry and Physics, 16, 5905–5931, 2016.

Niedermeier, D., Wex, H., Voigtländer, J., Stratmann, F., Brüggemann, E., Kiselev, A., Henk, H., and Heintzenberg, J.: LACIS-measurements and parameterization of sea-salt particle hygroscopic growth and activation, Atmospheric Chemistry and Physics, 8, 579–590, 2008.

Petters, M. and Kreidenweis, S.: A single parameter representation of hygroscopic growth and cloud condensation nucleus activity, Atmospheric Chemistry and Physics, 7, 1961–1971, 2007.

Poulain, L., Spindler, G., Birmili, W., Plass-Dülmer, C., Wiedensohler, A., and Herrmann, H.: Seasonal and diurnal variations of particulate nitrate and organic matter at the IfT research station Melpitz, Atmospheric Chemistry and Physics, 11, 12 579–12 599, doi:10.5194/acp-11-12579-2011, 2011.

Roberts, G. and Nenes, A.: A continuous-flow streamwise thermal-gradient CCN chamber for atmospheric measurements, Aerosol Science and Technology, 39, 206–221, 2005.

Schmale, J., Henning, S., Henzing, B., Keskinen, H., Sellegri, K., Ovadnevaite, J., Bougiatioti, A., Kalivitis, N., Stavroulas, L., Jefferson, A., Park, M., Schlag, P., Kristensson, A., Iwamotol, Y., Pringle, K., Reddington, C., Aalto, P., Aijala, M., Baltensperger, U., Bialek, J., Birmili, W., Bukowiecki, N., Ehn, M., Fjaeraa, A., Fiebig, M., Frank, G., Frohlich, R., Frumau, A., Furuyals, M., E. Hammerl', E. H., Heikkinen, L., Herrmann, E., Holzinger, R., Hyonols, H., Kanakidoug, M., Kiendler-Scharr, A., Kinouchi, K., Kos, G., Kulmala, M., Mihalopoulos, N., Motos, G., Nenes, A., O'Dowd, C., Paramonov, M., Petaja, T., Picard, D., Poulain, L., Prevot, A., Slowik, J., Sonntag, A., Swietlicki, E., Svenningsson, B., Tsurumaru, H., Wiedensohler, A., Wittbom, C., Ogren, J., Matsuki, A., Yum, S., Myhre, C., Carslaw, K., Stratmann, F., and Gysel, M.: Data Descriptor: Collocated observations of cloud condensation nuclei, particle size distributions, and chemical composition, Scientific Data, 4, doi:10.1038/sdata.2017.3, 2017.

Seifert, A. and Beheng, K.: A two-moment cloud microphysics parameterization for mixed-phase clouds. Part 1: Model description, Meteorology and Atmospheric Physics, 92, 45–66, doi:10.1007/s00703-005-0112-4, 2006.

Seinfeld, J. H. and Pandis, S. N.: Atmospheric Chemistry and Physics, Johl Wiley & Sons, Inc., New York, Chichester, Weinheim, Brisbane, Singapore, Toronto, 1326pp, 1998.

Siebert, H., Franke, H., Lehmann, K., Maser, R., Saw, E. W., Schell, D., Shaw, R. A., and Wendisch, M.: Probing Finescale Dynamics and Microphysics of Clouds with Helicopter-Borne Measurements, Bulletin of the American Meteorological Society, 87, 1727–1738, doi:10.1175/BAMS-87-12-1727, https://doi.org/10.1175/BAMS-87-12-1727, 2006.

Spindler, G., Gnauk, T., Grüner, A., Iinuma, Y., Müller, K., Scheinhardt, S., and Herrmann, H.: Size-segregated characterization of $PM_{10}$ at the EMEP site Melpitz (Germany) using a five-stage impactor: a six year study, Journal of Atmospheric Chemistry, 69, 127–157, 2012.

Spindler, G., Grüner, A., Müller, K., Schlimper, S., and Herrmann, H.: Long-term size-segregated particle ($PM_{10}$, $PM_{2.5}$, $PM_1$) characterization study at Melpitz - influence of air mass inflow, weather condition and season, Journal of Atmospheric Chemistry, 70, 165–195, 2013.

https://doi.org/10.5194/acp-2019-742
Preprint. Discussion started: 17 September 2019


Atmospheric Chemistry and Physics Discussions

Sudhakar, D., Quaas, J., Wolke, R., Stoll, J., Mühlbauer, A., Sourdeval, O., Salzmann, M., Heinold, B., and Tegen, I.: Implementation of aerosol-cloud interactions in the regional atmosphere-aerosol model COSMO-MUSCAT(5.0) and evaluation using satellite data, Geoscientific Model Development, 10, 2231–2246, doi:10.5194/gmd-10-2231-2017, 2017.

UBA: Kevin Hausmann, personal communication, 2017.

Wex, H., Petters, M., Carrico, C., Hallbauer, E., Massling, A., McMeeking, G., Poulain, L., Wu, Z., Kreidenweis, S., and Stratmann, F.: Towards closing the gap between hygroscopic growth and activation for secondary aerosol: Part 1 - Evidence from measurements, Atmospheric Chemistry and Physics, 9, 3987–3997, 2009.

Wex, H., McFiggans, G., Henning, S., and Stratmann, F.: Influence of the external mixing state of atmospheric aerosol on derived CCN number concentrations, Geophysical Research Letters, 37, doi: 10.1029/2010GL043 337, 2010.

Wolke, R., Schröder, W., Schrödner, R., and Renner, E.: Influence of grid resolution and meteorological forcing on simulated European air quality: A sensitivity study with the modeling system COSMO-MUSCAT, Atmospheric Environment, 53, 110–130, 2012.